JOURNAL OF VIROLOGY, July 1996, p. 4607–4616 Vol. 70, No. 7
0022-538X/96/$04.00+0

The GP64 Envelope Fusion Protein Is an Essential Baculovirus Protein Required for Cell-to-Cell Transmission of Infection

SCOTT A. MONSMA, A. G. P. OOMENS, AND GARY W. BLISSARD*

Boyce Thompson Institute, Cornell University, Ithaca, New York 14853-1801

Received 1 December 1995/Accepted 18 March 1996

To demonstrate the essential nature of the baculovirus GP64 envelope fusion protein (GP64 EFP) and to further examine the role of this protein in infection, we inactivated the *gp64 efp* gene of *Autographa californica* multicapsid nuclear polyhedrosis virus (Ac*M*NPV) and examined the biological properties of this virus in vivo. To provide GP64 EFP during construction of the recombinant GP64 EFP-null Ac*M*NPV baculovirus, we first generated a stably transfected insect cell line ($Sf9^{OP64\text{-}6}$) that constitutively expressed the GP64 EFP of *Orgyia pseudotsugata* multicapsid nuclear polyhedrosis virus (Op*M*NPV). The Ac*M*NPV *gp64 efp* gene was inactivated by inserting the bacterial *lacZ* gene in frame after codon 131 of the *gp64 efp* gene. The inactivated *gp64* gene was cloned into the Ac*M*NPV viral genome by replacement of the wild-type *gp64 efp* locus. When propagated in the stably transfected insect cells ($Sf9^{OP64\text{-}6}$ cells), budded virions produced by the recombinant Ac*M*NPV GP64 EFP-null virus (vAc^{64Z}) contained Op*M*NPV GP64 EFP supplied by the $Sf9^{OP64\text{-}6}$ cells. Virions propagated in $Sf9^{OP64\text{-}6}$ cells were capable of infecting wild-type Sf9 cells, and cells infected by vAc^{64Z} exhibited a blue phenotype in the presence of X-Gal (5-bromo-4-chloro-3-indolyl-β-D-galactopyranoside). Using cytochemical staining to detect vAc^{64Z} infected cells, we demonstrated that this GP64 EFP-null virus is defective in cell-to-cell propagation in cell culture. Although defective in cell-to-cell propagation, vAc^{64Z} produces occlusion bodies and infectious occlusion-derived virions within the nucleus. Occlusion bodies collected from cells infected by vAc^{64Z} were infectious to midgut epithelial cells of *Trichoplusia ni* larvae. However, in contrast to infection by a control virus, infection by vAc^{64Z} did not proceed into the hemocoel. Analysis of vAc^{64Z} occlusion bodies in a standard neonate droplet feeding assay showed no virus-induced mortality, indicating that occluded virions produced from vAc^{64Z} could not initiate a productive (lethal) infection in neonate larvae. Thus, GP64 EFP is an essential virion structural protein that is required for propagation of the budded virus from cell to cell and for systemic infection of the host insect.

Baculoviruses are large double-stranded DNA viruses that are pathogens of insects. Infection of the host begins when insect larvae acquire the virus orally. Infection is first observed in the epithelial cells of the midgut, and this is followed in most cases by systemic infection. One hallmark of the baculovirus infection cycle is the production of two structurally and functionally distinct virion phenotypes. One virion phenotype, the occlusion-derived virus (ODV), is found within the protective occlusion bodies. Once released from the occlusion body by the alkaline pH of the gut, the ODV initiates infection of the animal by infecting epithelial cells of the midgut. A second virion phenotype, the budded virus (BV), is produced by budding from the surfaces of infected cells. The BV is initially produced from infected midgut epithelial cells (12, 22) and is believed to be essential for systemic infection, mediating movement of the virus from the midgut to other tissues and propagating the infection from cell to cell within the infected animal. BVs are highly infectious to tissues of the hemocoel and to cultured cells, whereas ODVs appear to be less infectious in cell culture or when injected into the hemocoel (39, 40). The two virion phenotypes also differ in entry mechanisms, since the BVs enter cells via endocytosis (36), while the ODVs appear to fuse directly with the plasma membrane at the cell surface (12, 16).

The major envelope protein of the BV is the GP64 envelope fusion protein (GP64 EFP) (also known as GP67), which is an extensively processed type I integral membrane glycoprotein that has been studied in some detail (5, 8, 20, 25, 26, 28, 29, 35, 37, 41). Densely packed peplomers found on the surface of the BV are believed to be composed of the GP64 EFP protein (38), and these peplomers are acquired by the virion during budding. Recent studies of a soluble form of GP64 EFP indicate that the native form of GP64 EFP is trimeric (26), and thus, each peplomer is likely composed of a single trimer of GP64 EFP. The important role of GP64 EFP in BV infectivity is demonstrated by the neutralization of BV infectivity with antibodies specific to GP64 EFP (15, 25, 28, 38). By using syncytium formation assays and cells expressing GP64 EFP, it was shown that GP64 EFP is both necessary and sufficient for low-pH-activated membrane fusion activity (5, 25). In addition, two functional domains have been identified in GP64 EFP: (i) an oligomerization domain necessary for trimerization and transport and (ii) a small internal hydrophobic membrane fusion domain (25). Thus, functional studies of GP64 EFP show that GP64 EFP mediates membrane fusion in a pH-dependent manner, consistent with an essential role for GP64 EFP during viral entry by endocytosis.

While indirect data on the role of GP64 EFP in the infection cycle strongly suggest that GP64 EFP is essential for infectivity of the BV, conclusive data have been lacking. No temperature-sensitive mutants with mutations in the GP64 EFP gene are known, and previous attempts to generate a helper-independent virus containing a GP64 EFP deletion were unsuccessful (24a). To demonstrate the essential nature of GP64 EFP and to further characterize the role of GP64 EFP in infection, we generated a stably transfected cell line that constitutively expresses the GP64 EFP of *Orgyia pseudotsugata* multicapsid

* Corresponding author. Mailing address: Boyce Thompson Institute, Cornell University, Tower Rd., Ithaca, NY 14853-1801. Phone: (607) 254-1366. Fax: (607) 254-1242. Electronic mail address: gwb1@cornell.edu.

nuclear polyhedrosis virus (Op*M*NPV) and used the cell line to generate a recombinant GP64 EFP-null *Autographa californica* multicapsid nuclear polyhedrosis virus (Ac*M*NPV) baculovirus. We then examined the effect of the GP64 EFP-null mutation on viral transmission in both cell culture and insect larvae.

MATERIALS AND METHODS

Cells, insects, and antibodies. For production of stably transfected cell lines and propagation of Ac*M*NPV, *Spodoptera frugiperda* Sf9 cells were cultured in TNM-FH complete medium containing 10% fetal bovine serum at 27°C (14, 32). For neonate and larval bioassays, larvae of *Trichoplusia ni* were reared as described previously (18). Monoclonal antibody (MAb) AcV5 (15) was used to detect GP64 EFP of both Ac*M*NPV and Op*M*NPV. MAb OpE4A was raised against a purified soluble form of Op*M*NPV GP64 EFP (GP64 EFP^{sol}) (26). Because OpE4A recognizes both native and denatured forms of Op*M*NPV GP64 EFP and does not cross-react with GP64 EFP of Ac*M*NPV, OpE4A was used to distinguish between Op*M*NPV and Ac*M*NPV GP64 EFPs. MAb 39 (42) was used to detect the Ac*M*NPV capsid protein, P39. A commercially available anti-β-galactosidase MAb (Promega) was used to detect the GP64–β-galactosidase fusion protein. A rabbit polyclonal antiserum was also generated against purified soluble Op*M*NPV GP64 EFP (GP64 EFP^{sol}) (26). The anti-GP64 EFP^{sol} antiserum reacts with both sodium dodecyl sulfate (SDS)-denatured and native GP64 EFPs of both Op*M*NPV and Ac*M*NPV.

Virus preparation. Viral DNA used for the generation of recombinant viruses was prepared from the E2 strain of Ac*M*NPV (30) by standard methods (27). For production of BV stocks and occlusion bodies of the wild-type and recombinant viruses, cells (Sf9 or Sf9$^{OP64\text{-}6}$ cells [see below]) were infected at a multiplicity of infection (MOI) of 0.1 and incubated at 27°C for 5 to 7 days. Supernatants were harvested, and titers were determined by end-point dilution. The titers of recombinant Ac*M*NPV virus lacking *gp64* expression were determined on the Sf9$^{OP64\text{-}6}$ cells, and those of the wild-type Ac*M*NPV virus and recombinant virus vAc^{hsZ} were determined on Sf9 cells. Occlusion bodies were purified from infected cells by sequential washing with 0.5% SDS, 0.5 M NaCl, and distilled water as described previously (27). For analysis of BV structural proteins, BVs were isolated from viral stocks by pelleting through a 25% sucrose pad and then by centrifugation on 25 to 60% sucrose gradients (27). The BV band was collected, diluted in phosphate-buffered saline (PBS) (pH 6.2), pelleted, and resuspended in SDS lysis buffer for SDS-polyacrylamide gel electrophoresis (SDS-PAGE) on 10% acrylamide gels.

Isolation of stably transfected insect cell lines expressing Op*M*NPV GP64 EFP. To generate stably transfected insect cells, Sf9 cells were transfected with two plasmids. One plasmid (p64-166 [5]) encodes the Op*M*NPV *gp64 efp* open reading frame (ORF) under the control of its own 166-bp promoter. The second plasmid (pAc ie1-Neo) encodes a bacterial neomycin resistance gene under the control of the Ac*M*NPV *ie1* promoter and was constructed by using the approach described by Jarvis et al. (19). Transfection and G418 selection were performed essentially as described previously (21, 31). Briefly, Sf9 cells were plated at a density of 10^6 cells per well (34-mm diameter). The cells were transfected with 2 μg of p64-166 plasmid plus 1 μg of pAc ie1-Neo by calcium phosphate precipitation (32). One day after transfection, the cells were replated at low density in 75-cm^2 flasks and maintained for 2 weeks in TNM-FH complete medium containing 1 mg of G418 (Geneticin; GIBCO-BRL) per ml. During this period, mock-transfected Sf9 control cells died as a result of the G418 selection. The G418-resistant transfected cells were replated in TNM-FH complete medium (lacking G418) at a low density. Single colonies were isolated and transferred to individual wells of a 24-well plate. Isolated lines were screened for GP64 EFP expression by cell surface staining of paraformaldehyde-fixed cells with MAb AcV5 and an alkaline phosphatase-conjugated goat anti-mouse secondary antibody. Isolated lines were also screened for GP64 EFP fusion activity by a syncytium formation assay (5, 25).

Quantification and analysis of GP64 EFP expression in stably transfected cell lines. To analyze GP64 EFP expression in stably transfected cell lines, we quantified the levels of GP64 EFP expressed in stably transfected Sf9 cells, transiently transfected Sf9 cells, and Ac*M*NPV-infected Sf9 cells, using quantitative enhanced chemiluminescence (ECL)-Western blots (immunoblots), cell surface enzyme-linked immunosorbent assay (CELISA), and flow cytometry. For all three assays, the following cells were analyzed under the following conditions: (i) two cell lines (Sf9$^{OP64\text{-}6}$ and Sf9$^{OP64\text{-}2}$) constitutively expressing Op*M*NPV GP64 EFP were plated at passage 39 and analyzed at 44 h after being plated, (ii) Sf9 cells transfected with plasmid p64-166 (encoding Op*M*NPV GP64 EFP) at 3.75 μg of plasmid per 3×10^5 cells were analyzed at 44 h posttransfection, (iii) Sf9 cells infected with Ac*M*NPV (MOI, 10) were analyzed at 24 h postinfection (p.i.), and (iv) Sf9 cells were analyzed at 44 h after plating as a negative control. Values for this negative control were subtracted as background in quantitative analysis of CELISA and ECL-Western blots.

Quantitative ECL-Western blot analyses were performed by comparison of cell lysates with a standard dilution series of purified GP64 EFP^{sol}, using MAb AcV5 to detect GP64 EFP and GP64 EFP^{sol}. A preparation of GP64 EFP^{sol} (purity of >95% as judged by SDS-PAGE and Coomassie blue staining) was quantified by measurements of A_{280}. The predicted molar extinction coefficient of pure, native GP64 EFP^{sol} at 280 nm was calculated as 77,510 M^{-1} cm^{-1} on the basis of the predicted amino acid content of 14 Cys, 11 Trp, and 11 Tyr residues per molecule (11). The molecular mass of mature GP64 EFP^{sol} predicted from the amino acid sequence is 52,519 Da (amino acids 18 to 477 of Op*M*NPV GP64 EFP). To prepare a standard curve, purified GP64 EFP^{sol} was added to Sf9 cell lysates in SDS lysis buffer (30,960 cells per 20 μl of lysate) at concentrations of 0.1 to 40 ng of GP64 EFP^{sol} per 20 μl of lysate (equivalent to 1.3×10^4 to 5×10^6 trimers of GP64 EFP^{sol} per cell). Triplicate cell samples and standard curve samples were electrophoresed on SDS-PAGE gels and blotted to polyvinylidene difluoride membranes, and GP64 EFP was detected with MAb AcV5 by ECL (Amersham). For quantification of films by densitometry, ECL exposure times were chosen to avoid film saturation. Exposed films were digitized on a flat-bed scanner, and the ECL signals (below saturation) were quantified with Image-quant software (Molecular Dynamics). Quantitative measurements of GP64 EFP expression from the samples of infected, transiently transfected, or stably transfected cells were performed by comparison of the mean ECL signal with the GP64 EFP^{sol} standard curve. The mean ECL signal from each triplicate cell sample was divided by the estimated number of cells in the sample, which was determined by counting the cells present in triplicate wells of an identically treated replicate plate. Conversion from nanograms of GP64 EFP^{sol} per cell to trimers per cell used the predicted mass of GP64 EFP^{sol}: (52,519 g/mol)/(6.02×10^{23} molecules per mol) = 8.72×10^{-20} g per GP64 EFP^{sol} molecule = 2.62×10^{-19} g per GP64 EFP^{sol} trimer. Because both GP64 EFP^{sol} and GP64 EFP were detected with a MAb that recognizes a single defined epitope (25), the ECL signal is proportional to the number of molecules rather than to the mass.

Relative levels of GP64 EFP localized on the cell surface were determined by a previously described CELISA technique (25) with minor modifications. Cells were fixed for 10 min at room temperature (RT) with 0.5% glutaraldehyde in PBS (pH 7.4), and surface GP64 EFP was detected with MAb AcV5. The mean CELISA signal from each triplicate cell sample was normalized to the estimated number of cells per well, determined as described above for quantitative ECL analysis.

To examine the variation of GP64 EFP surface density in populations of cells, uninfected Sf9 cells, Ac*M*NPV-infected Sf9 cells, the stably transfected cell lines, and transiently transfected Sf9 cells were analyzed by flow cytometry with anti-GP64 EFP^{sol} antiserum. For flow cytometry, cells were gently suspended in TNM-FH complete medium containing 0.02% (wt/vol) sodium azide (NaN_3) and incubated for 20 min at RT. Cells (10^6 cells per 250 μl) were incubated with anti-GP64 EFP^{sol} antiserum (diluted 1:20,000 in binding buffer; binding buffer is PBS [pH 7.0] containing 1% [wt/vol] gelatin and 0.02% NaN_3) for 40 min at RT. The cells were washed twice with PBS-NaN_3 (PBS [pH 7.0] containing 0.02% NaN_3) and then incubated with a fluorescein isothiocyanate-conjugated goat anti-rabbit secondary antibody (diluted 1:100 in binding buffer) (Pierce). Cells were washed four times in PBS-NaN_3 and resuspended in 350 μl of PBS-NaN_3 for flow cytometry. For each cell type, control samples were incubated without antibodies or with only the secondary antibody. Fluorescence was analyzed by flow cytometry (EPICS; Coulter Corp.), and fluorescence data were collected for 10^4 cells from each sample. Dead cells were excluded from analysis by gating of the live cell population on the basis of the ratio of forward to side scatter.

Generation of a GP64 EFP-null Ac*M*NPV baculovirus. To construct a transfer vector for allelic replacement of the *gp64 efp* locus of the Ac*M*NPV genome, the 4,718-bp *Eco*RI-*Sma*I fragment (corresponding to nucleotides 107,326 to 112,043 from the *Eco*RI H fragment [1]) of Ac*M*NPV strain E2 was cloned into the pBS vector (Stratagene) to generate the plasmid pAcEcoHΔSma. This plasmid contains 2,327 bp upstream of the *gp64 efp* ORF, the *gp64 efp* ORF, and 853 bp downstream of the *gp64 efp* ORF. To disrupt the Ac*M*NPV *gp64 efp* gene by insertional mutagenesis, we generated an in-frame fusion between gp64 efp and the *Escherichia coli lacZ* gene in an Ac*M*NPV GP64 EFP expression plasmid, pAcNru(BKH). The pAcNru(BKH) expression plasmid contains an 18-bp in-frame linker encoding unique *Bgl*II, *Kpn*I, and *Hin*dIII restriction sites, inserted at the *Nru*I restriction site within the *gp64 efp* ORF of plasmid p166B+1 Ac Spe/Bgl (25). A 3,072-bp *Bam*HI fragment containing the *lacZ* ORF (derived from pMC1871 [7]) was subcloned into *Bgl*II-digested pAcNru(BKH). The resulting construct [pAcNru(lacZ)] contains a *gp64-lacZ* fusion after codon 131 of *gp64 efp* (3, 41), and the fusion gene ORF terminates at the end of the *lacZ* insertion. The 3,447-bp *Bsm*I-*Sac*II fragment of pAcNru(lacZ) (containing the *lacZ* cassette and the flanking portions of *gp64 efp*) was subcloned into *Bsm*I-*Sac*II-digested pAcEcoHΔSma, to generate plasmid pAcGP64Z (see Fig. 2A). Finally, to ensure inactivation of the *gp64 efp* gene, the downstream portion of the *gp64 efp* ORF was truncated by digesting pAcGP64Z with *Nco*I, removing the resulting 54-bp *Nco*I-*Nco*I fragment, and then blunting and religating to generate pAcGP64ZΔNco. This deletion results in a frameshift mutation and terminates the *gp64 efp* ORF after codon 452, 30 codons upstream of the predicted transmembrane domain. Recombinant viruses were generated by standard protocols (27), by cotransfecting viral DNA from wild-type Ac*M*NPV strain E2 and pAcGP64ZΔNco plasmid DNA into the GP64 EFP-expressing Sf9$^{OP64\text{-}6}$ cells. A recombinant virus (vAc^{64Z}) was isolated from the culture supernatant by plaque purification on Sf9$^{OP64\text{-}6}$ cells, using X-Gal (5-bromo-4-chloro-3-indolyl-β-D-galactopyranoside) in the agarose overlay to identify the recombinant plaques.

The structure of the *gp64 efp* locus in vAc^{64Z} was analyzed by PCR amplification and restriction mapping. DNA was extracted from infected Sf9 cells at 24

h p.i., or viral DNA was isolated from BV pelleted through a 25% sucrose cushion (27). For PCR analysis, the following primers, homologous to the 5′ and 3′ ends, respectively, of the *gp64 efp* ORF, were used (see Fig. 2A): GB111 (5′-GAGCTGATCGACCGTTGGGG-3′) and GB152 (5′-CGGTTTCTGATC ATACAGTACA-3′). To verify the presence of the *Nco*I deletion in vAc^{64Z}, PCR amplification was performed with primers flanking the deletion site (see Fig. 2A): GB53 (5′-CCAGCGGCTGGTCGTTTATCGCCC-3′) and GB152.

For comparisons of infection in Sf9 cells and *T. ni* larvae, a control virus (vAc^{hsZ}; kindly provided by P. Roelvink) was used. vAc^{hsZ} contains the bacterial *lacZ* gene (under the control of the *Drosophila hsp70* promoter) in the *p10* locus and lacks a functional *p10* gene (vAc^{hsZ} is identical to recombinant virus AcNPV/As3 [34]).

Assays. (i) Cell-to-cell transmission in cell culture. To monitor the cell-to-cell transmission of infection in cell culture, Sf9 cells were infected at an MOI of 0.1 with vAc^{64Z} or vAc^{hsZ}. After a 1-h incubation at RT, the inoculum was removed and the cells were rinsed twice with complete TNM-FH medium and then placed in complete TNM-FH medium and incubated at 27°C. At 20, 48, and 72 h p.i., the cells were fixed and stained for β-galactosidase activity to detect cells infected by the *lacZ*-marked viruses (33).

(ii) Larval feeding assays. Neonate bioassays were performed by the droplet feeding assay (18), using occlusion bodies prepared either from wild-type-Ac*M*NPV-infected Sf9 cells or from vAc^{64Z}-infected Sf9^{OP64-6} cells. Occlusion bodies were suspended in distilled water, counted in a hemacytometer, and then diluted to various concentrations in distilled water containing blue food coloring. After the droplet feeding, larvae that had imbibed were identified by their blue color and were placed in individual cups with an artificial diet and maintained at 29°C in darkness. Because a low level of nonviral neonate mortality is sometimes observed, larvae that died within the first 24 h after feeding were discarded from the analysis. Virus-induced mortality was scored at 4 days postfeeding. For late larval bioassays, newly molted fourth-instar *T. ni* larvae were starved for 1.5 to 2 h after molting and then fed occlusion bodies prepared from either vAc^{64Z}-infected Sf9^{OP64-6} cells or vAc^{hsZ}-infected Sf9 cells. Each larva was fed 1 μl of a suspension containing 1,000 occlusion bodies per μl, 5% (wt/vol) sucrose, and blue food coloring. The larvae were kept in empty cups for 2 h after feeding and then were placed in individual cups with an artificial diet and maintained at 27°C in darkness. At various times postfeeding, larvae were dissected in PBS (pH 7.4) by a single longitudinal incision through the dorsal cuticle and pinned to expose the gut and hemocoel. Dissected larvae were fixed for 30 min at RT by immersion in 0.01% (wt/vol) glutaraldehyde–2% (wt/vol) paraformaldehyde in PBS (pH 7.4). After fixation, the larvae were rinsed three times for 5 min in PBS (pH 7.4) and stained with X-Gal (1 mg/ml) in PBS (pH 7.4) containing 3 mM $K_3Fe(CN)_6$ and 3 mM $K_4Fe(CN)_6$ (10). Staining times were typically 2 h at RT (for Fig. 5A, C, and D), but they were extended to 18 h at RT to verify the lack of systemic infection with vAc^{64Z} (for Fig. 5B).

RESULTS

Generation of stably transfected cell lines. Because previous studies using anti-GP64 EFP antibodies suggested that GP64 EFP might be an essential component of BVs, we used a strategy in which the GP64 EFP protein was provided in *trans*, to complement the inactivation of the *gp64 efp* gene in the virus. To provide GP64 EFP in *trans*, a stably transfected cell line that constitutively expresses the Op*M*NPV GP64 EFP protein was generated by cotransfection with plasmids encoding GP64 EFP and the bacterial neomycin resistance gene, followed by selection for G418 resistance. To express the Op*M*NPV GP64 EFP, we used a GP64 EFP expression plasmid (p64-166) (5) that contains the Op*M*NPV *gp64 efp* ORF under control of an Op*M*NPV *gp64 efp* early promoter construct that has been studied in detail (2, 4, 23, 24). Transfected Sf9 cells that were resistant to G418 were selected, and isolated cell lines were established.

Quantitative analysis of GP64 EFP expression in stably transfected cell lines. Expression of GP64 EFP from two stably transfected cell lines (Sf9^{OP64-6} and Sf9^{OP64-2}) was compared with that from Ac*M*NPV-infected Sf9 cells (at 24 h p.i.) and with transient GP64 EFP expression from Sf9 cells transfected with plasmid p64-166 (at 44 h posttransfection). For these analyses, we used several quantitative techniques to determine the absolute and relative levels of GP64 EFP: (i) absolute levels of GP64 EFP from whole cells were determined by quantitative ECL-Western blots, (ii) relative surface levels of GP64 EFP were determined by CELISA, and (iii) the variation in the average surface density of GP64 EFP was determined by flow cytometry (Fig. 1).

A soluble secreted form of GP64 EFP (GP64 EFP^{sol}) was used to generate a standard curve for quantitative ECL analysis (see Materials and Methods) (Fig. 1A, inset). Comparisons of GP64 EFP present in the whole-cell extracts from transiently transfected Sf9 cells, Ac*M*NPV-infected Sf9 cells, and two stably transfected cell lines are shown in Fig. 1A. The quantity of GP64 EFP detected in Ac*M*NPV-infected Sf9 cells at 24 h p.i. corresponds to approximately 1.3×10^6 trimers of GP64 EFP per cell. The quantity of GP64 EFP detected in the stably transfected line Sf9^{OP64-6} (2.5×10^5 trimers per cell) was approximately 19% of that detected in Ac*M*NPV-infected cells at 24 h p.i. The total GP64 EFP levels from line Sf9^{OP64-2} were lower (1.6×10^5 trimers per cell), corresponding to approximately 12% of that detected in Ac*M*NPV-infected cells. Interestingly, transiently transfected Sf9 cells assayed at 44 h posttransfection (included as a control) showed the highest average levels of GP64 EFP expression, approximately 3.2×10^6 trimers per cell, or 2.5 times that detected in Ac*M*NPV-infected Sf9 cells.

Detection and quantification (by CELISA) of the average relative levels of surface-localized GP64 EFP (Fig. 1B) showed that the level of surface-localized GP64 EFP from Sf9^{OP64-6} cells was similar to that from Ac*M*NPV-infected Sf9 cells at 24 h p.i., a time when virion budding is occurring. The average surface levels of GP64 EFP on Sf9^{OP64-2} cells were lower, corresponding to approximately 70% of that detected on Ac*M*NPV-infected Sf9 cells or Sf9^{OP64-6} cells. Transiently transfected Sf9 cells assayed at 44 h posttransfection expressed the highest average levels of surface GP64 EFP, corresponding to approximately 2.7 times that detected on Ac*M*NPV-infected Sf9 cells at 24 h p.i.

Because GP64 EFP expression levels may vary between individual cells in a population, we also used flow cytometry to determine the degree of variation. The degrees of variation (of GP64 EFP surface densities) within populations were compared for Ac*M*NPV-infected Sf9 cells at 24 h p.i., stably transfected cell lines Sf9^{OP64-6} and Sf9^{OP64-2}, and transiently transfected cells at 44 h posttransfection (Fig. 1C to G). Analysis of cells from each population showed that both stably transfected cell lines (Sf9^{OP64-6} and Sf9^{OP64-2}) and transiently transfected Sf9 cells contain a significantly wider variation in GP64 EFP surface densities than do Ac*M*NPV-infected Sf9 cells, as indicated by the broader peaks (compare Fig. 1E, F, and G with Fig. 1D). A small proportion of cells in both of the stably transfected cell populations and in the transiently transfected cell population showed higher levels of surface GP64 EFP (relative fluorescence intensities of approximately 200 to 300) than did infected Sf9 cells (maximum fluorescence intensity of approximately 150).

Thus, by several measurements, the average surface density of GP64 EFP on stably transfected Sf9^{OP64-6} cells appears to be comparable to that on Ac*M*NPV-infected Sf9 cells at 24 h p.i., a time at which active budding of virions is occurring. Therefore, the level of GP64 EFP expressed by Sf9^{OP64-6} cells was judged to be sufficient to complement inactivation of the *gp64 efp* gene in the Ac*M*NPV viral genome.

Generation of vAc^{64Z}. To inactivate the *gp64 efp* gene in Ac*M*NPV, we used insertional mutagenesis. The Ac*M*NPV *gp64 efp* gene was inactivated by inserting the bacterial *lacZ* ORF (in frame) into the *gp64 efp* ORF after codon 131 (Fig. 2A). Although the *lacZ* ORF contains a translation termination codon, we also created a frameshift mutation after codon 452 of *gp64 efp*, by removing a 54-bp *Nco*I restriction fragment. This frameshift resulted in a translation termination codon

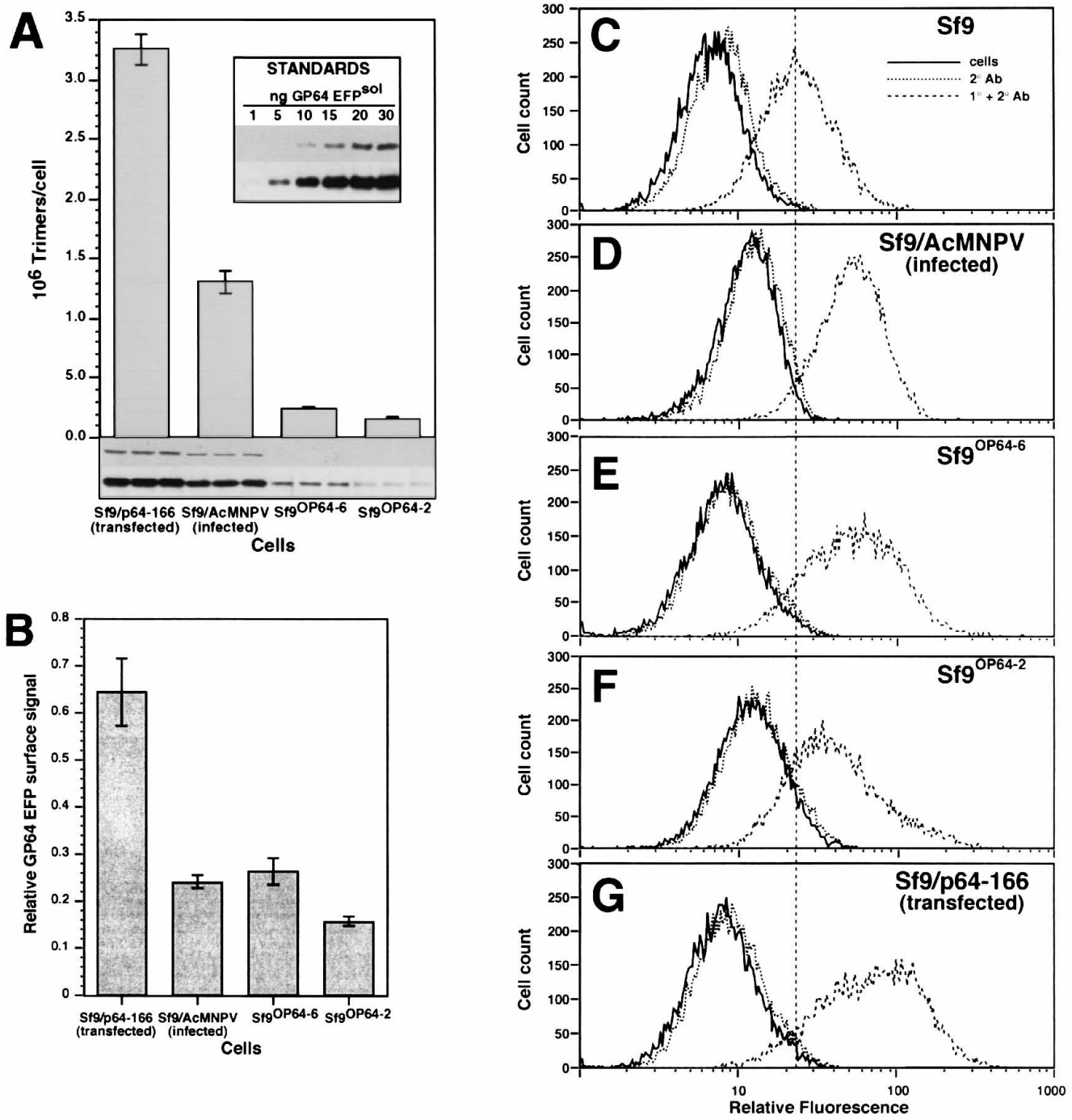

FIG. 1. Expression of GP64 EFP by transiently transfected Sf9 cells (transfected), Ac*M*NPV-infected Sf9 cells (infected), and two stably transfected Sf9 cell lines (Sf9^{OP64-6} and Sf9^{OP64-2}). For analysis of infected cells, Sf9 cells were infected with wild-type Ac*M*NPV at an MOI of 10 and analyzed at 24 h p.i. Transiently transfected cells were transfected with plasmid p64-166 (encoding Op*M*NPV GP64 EFP) and analyzed at 44 h posttransfection. Stably transfected cell lines Sf9^{OP64-6} and Sf9^{OP642} were analyzed at 44 h after plating. (A) ECL-Western blot quantification of total GP64 EFP. Cell lysates were prepared from triplicate samples of each cell type and analyzed by Western blotting with ECL detection using MAb AcV5. Two exposures of the triplicate samples of each cell type are shown below the graph. Absolute quantities of GP64 EFP per cell were determined by densitometry and extrapolation from a standard curve prepared with purified GP64 EFP^{sol} (inset). The inset shows two exposures of a series of standard concentrations (in nanograms per 20 μl) of GP64 EFP^{sol}. Each bar in the graph represents the calculated mean number of GP64 EFP trimers per cell; error bars represent the standard deviations for triplicate samples for each indicated cell type. All data were normalized to those for Sf9 cells analyzed at 44 h after plating. (B) CELISA of surface-localized GP64 EFP. Relative levels of surface-localized GP64 EFP were determined by CELISA of glutaraldehyde-fixed cells with MAb AcV5. Each bar represents the mean CELISA signal for triplicate samples, normalized to the estimated mean number of cells present in each sample. Error bars represent the standard deviations for triplicate samples for each indicated cell type. All data were normalized to those for Sf9 cells analyzed at 44 h after plating. (C to G) Flow cytometry analysis of surface-localized GP64 EFP on individual cells. Unfixed cells from each indicated population were incubated with an anti-GP64 EFP^{sol} polyclonal serum in the presence of sodium azide. Bound antibodies were detected with a fluorescein isothiocyanate-conjugated secondary antibody (2° Ab). Each graph plots the cell count versus the relative fluorescence level. For each population, samples analyzed included cells incubated without antibodies, cells incubated with the secondary antibody only, and cells incubated with both primary and secondary antibodies. For reference, the mean fluorescence intensity for the negative control (Sf9 cells incubated with the anti-GP64 EFP primary antibody and the fluorescein isothiocyanate-conjugated secondary antibody) is indicated by the vertical dashed line.

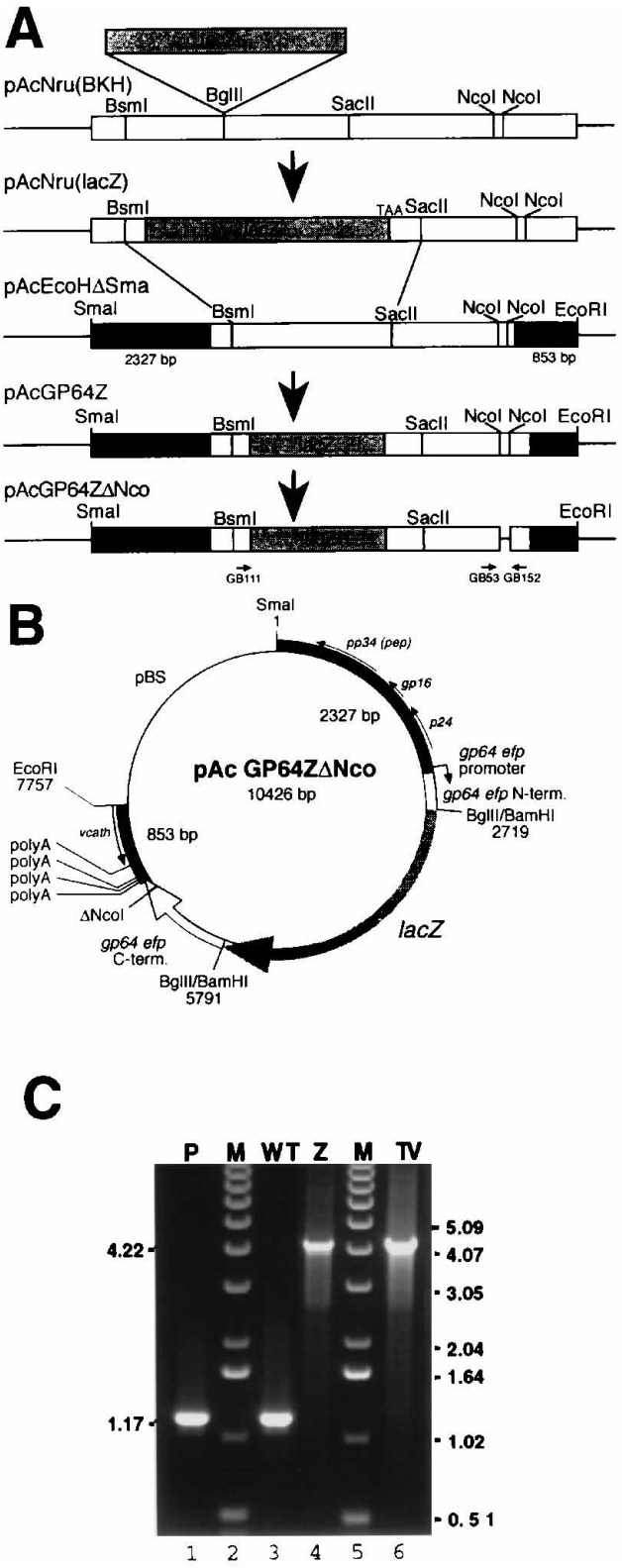

FIG. 2. Insertional mutagenesis of the Ac*M*NPV *gp64 efp* gene. (A) Construction of the *gp64-lacZ* transfer vector pAcGP64ZΔNco. Plasmid names are indicated for each construct (diagrams are not to scale). The *lacZ* ORF is shaded, the *gp64 efp* ORF is indicated in white, and Ac*M*NPV sequences flanking the *gp64 efp* ORF are indicated in black. The small arrows below the bottom diagram indicate the locations of primers (GB111, GB53, and GB152) used for PCR analysis. (B) Map of the *gp64-lacZ* transfer vector pAcGP64ZΔNco. The transfer vector contains 2,327 bp of flanking sequences upstream of the *gp64 efp* ORF and 853 bp of flanking sequences downstream of the wild-type *gp64 efp* stop codon. Also indicated are the locations and orientations of genes flanking the *gp64 efp* locus (*vcath*, *p24*, *gp16*, and *pp34* [*pep*]). (C) PCR amplification of the *gp64 efp* locus of wild-type Ac*M*NPV or vAc^{64Z}. Primers flanking the *lacZ* insertion (GB111 and GB152 [see panel A) were used to amplify the *gp64 efp* locus. The templates used for PCR amplification were plasmid DNA containing a wild-type Ac*M*NPV *gp64 efp* gene (P), DNA extracted from Sf9 cells infected with wild-type Ac*M*NPV (WT), DNA extracted from Sf9 cells infected with vAc^{64Z} (Z), and plasmid DNA from the transfer vector pAcGP64ZΔNco (TV). The intact *gp64 efp* ORF is predicted to yield a 1.17-kb PCR product, while the disrupted *gp64 efp* ORF resulting from *lacZ* insertion and the *Nco*I deletion is predicted to yield a 4.22-kb product. Lanes 2 and 5 contain molecular size standards (M), indicated on the right in kilobase pairs.

immediately upstream of the GP64 EFP transmembrane domain and ensured inactivation of the *gp64 efp* gene. The *gp64-lacZ* fusion gene was then cloned into a transfer vector containing sequences flanking the *gp64 efp* locus in Ac*M*NPV (Fig. 2B) (pAcGP64ZΔNco). Recombination of this transfer vector into the *gp64 efp* locus of wild-type Ac*M*NPV results in a virus wild type for all genes except *gp64 efp*. To generate recombinant viruses defective for GP64 EFP, transfections, recombination, and viral growth were carried out with the $Sf9^{OP64\text{-}6}$ cell line. A recombinant virus (vAc^{64Z}) was isolated by plaque purification on $Sf9^{OP64\text{-}6}$ cells, using X-Gal in the plaque overlay to detect β-galactosidase expression. Although the *gp64 efp* promoter is active in both early and late phases of infection, β-galactosidase activity was not detectable before 5 to 7 days p.i., unless the plaque assay plates were subjected to a freeze-thaw cycle to disrupt the infected cells. This result suggested that active GP64–β-galactosidase fusion protein was not secreted into the medium, despite the presence of the GP64 EFP signal peptide in the GP64–β-galactosidase fusion protein.

To confirm the location of the *gp64-lacZ* insertion in vAc^{64Z}, the *gp64 efp* locus of the vAc^{64Z} recombinant virus was examined by PCR amplification with primers complementary to the 5′ and 3′ ends of the *gp64 efp* gene (Fig. 2A) (GB111 and GB152). As control templates for PCR, we used a plasmid containing the wild-type Ac*M*NPV *gp64 efp* gene (negative control), DNA from cells infected with wild-type Ac*M*NPV, or plasmid DNA of the transfer vector pAcGP64ZΔNco (positive control). Amplification from the plasmid containing the wild-type *gp64 efp* gene or Ac*M*NPV viral DNA resulted in a 1.17-kb product, as predicted from the sequence (Fig. 2C, lanes 1 and 3). Amplification from the pAcGP64ZΔNco transfer vector or DNA from cells infected by vAc^{64Z} resulted in a single 4.22-kb product, as predicted from allelic replacement of the *gp64 efp* locus by the *gp64-lacZ* fusion gene (Fig. 2C, lanes 4 and 6). PCR analysis (with primers GB53 and GB152 [Fig. 2A]) was also used to verify that the recombinant virus vAc^{64Z} lacked the *Nco*I fragment deleted from the downstream region of the *gp64 efp* ORF (data not shown). The structure of the recombinant virus vAc^{64Z} was also examined by restriction enzyme digestion of viral genomic DNA. As expected, the *Eco*RI-*Bam*HI restriction profile of vAc^{64Z} differed from that of wild-type Ac*M*NPV only in the *Eco*RI H and *Bam*HI G fragments, confirming replacement of the *gp64 efp* locus (data not shown). Thus, PCR analysis, restriction mapping, and β-galactosidase activity indicate that the recombinant virus vAc^{64Z} contains only the *gp64-lacZ* fusion gene in the *gp64 efp* locus, and cells infected with vAc^{64Z} express β-galactosidase activity.

To verify that the *gp64 efp* gene was inactivated, vAc^{64Z}-infected Sf9 cells were examined by ECL-Western blot analysis (Fig. 3A). Cells were infected with either vAc^{64Z} or wild-type Ac*M*NPV, and cell lysates were prepared at 24 and 48 h p.i.

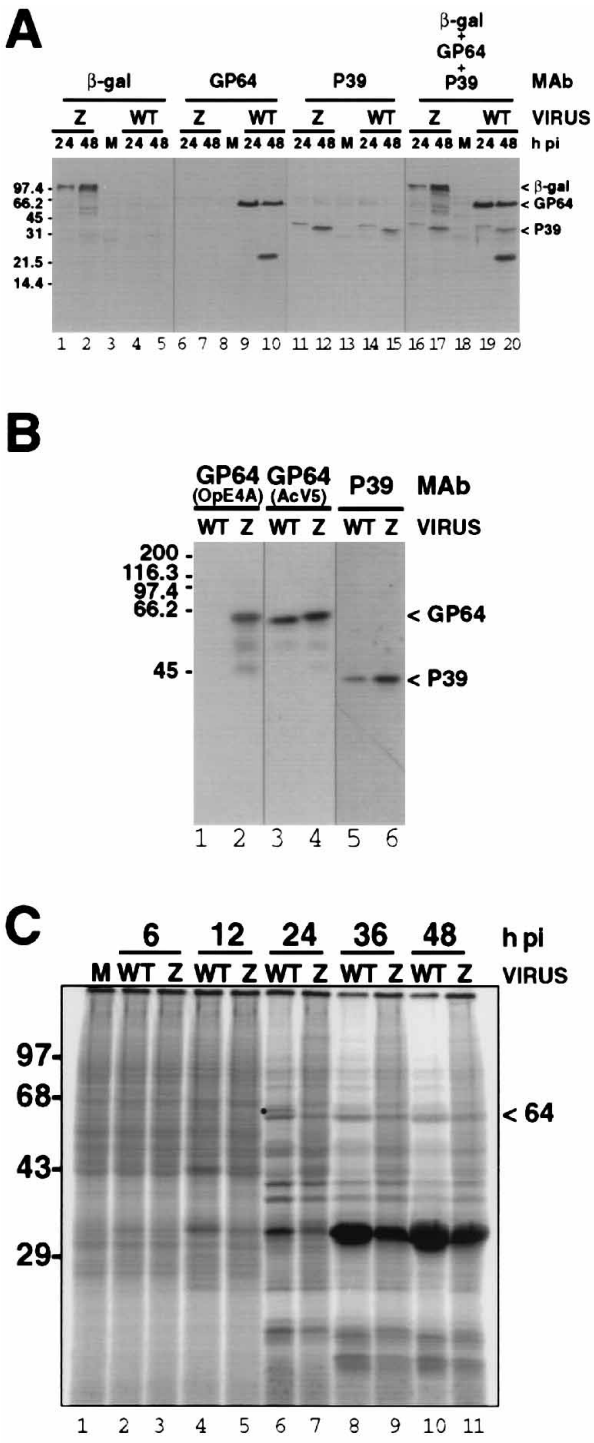

FIG. 3. Analysis of GP64 EFP in infected Sf9 cells (A) and purified BVs (B) and protein synthesis in infected Sf9 cells (C). (A) Western blot analysis of expression of the GP64–β-galactosidase fusion protein (β-gal), GP64 EFP (GP64), and the major capsid protein (P39) in Sf9 cells infected with either vAc^{64Z} (Z) or wild-type Ac*M*NPV (WT). Sf9 cells were infected at an MOI of 10 with vAc^{64Z} (lanes 1, 2, 6, 7, 11, 12, 16, and 17) or with wild-type Ac*M*NPV (lanes 4, 5, 9, 10, 14, 15, 19, and 20); mock-infected cells (M) were included as a negative control (lanes 3, 8, 13, and 18). Cell lysates were prepared for SDS-PAGE and Western blot analysis at 24 h p.i. (lanes 1, 4, 6, 9, 11, 14, 16, and 19) or 48 h p.i. (lanes 2, 5, 7, 10, 12, 15, 17, and 20). Replicate blots were probed with either a MAb directed against *E. coli* β-galactosidase (lanes 1 to 5); MAb AcV5, which is directed against GP64 EFP (lanes 6 to 10); or MAb 39, which is directed against P39 capsid protein (lanes 11 to 15). Lanes 16 to 20 were probed with a mixture of all three MAbs. Bound antibodies were detected by ECL. Positions of protein size standards are indicated on the left in kilodaltons. (B) Detection of Op*M*NPV GP64 EFP on vAc^{64Z} BVs. BVs were purified from supernatants of Ac*M*NPV-infected Sf9 cells (lanes 1, 3, and 5) or vAc^{64Z}-infected $Sf9^{OP64\text{-}6}$ cells (lanes 2, 4, and 6) by centrifugation on 25 to 60% sucrose gradients. The BV bands were collected and analyzed by SDS-PAGE and Western blotting. Duplicate blots were probed with MAb OpE4A, which recognizes only the GP64 EFP of Op*M*NPV (lanes 1 and 2); with MAb AcV5, which recognizes the GP64 EFPs of both AcMNPV and OpMNPV (lanes 3 and 4); or with MAb 39, which recognizes the P39 capsid protein (lanes 5 and 6). Bound antibodies were detected by ECL. Positions of protein size standards are indicated on the left in kilodaltons. (C) Kinetics of infection-specific protein expression. Sf9 cells were infected at an MOI of 20 with either vAc^{64Z} (lanes 3, 5, 7, 9, and 11) or wild-type Ac*M*NPV (lanes 2, 4, 6, 8, and 10). At the indicated times p.i., the cells were pulse-labeled for 2 h with [^{35}S]methionine. As a negative control, mock-infected cells (M) were labeled at the first time point (lane 1). After the labeling period, the cells were lysed and labeled proteins were analyzed by SDS-PAGE and PhosphorImager analysis. Positions of protein size standards are indicated on the left in kilodaltons.

Replicate blots were probed with MAbs specific to β-galactosidase (Fig. 3A, lanes 1 to 5), GP64 EFP (Fig. 3A, lanes 6 to 10), or P39 capsid protein (Fig. 3A, lanes 11 to 15). A replicate blot was also probed with a mixture of all three antibodies (Fig. 3A, lanes 16 to 20). Expression of β-galactosidase was detected only in cells infected with vAc^{64Z} (Fig. 3A, lanes 1 and 2) and not in cells infected with wild-type Ac*M*NPV (Fig. 3A, lanes 4 and 5). GP64 EFP expression was not detectable in cells infected with vAc^{64Z} (Fig. 3A, lanes 6 and 7). However, expression of the capsid protein P39 was detected in cells infected with either vAc^{64Z} or wild-type Ac*M*NPV (Fig. 3A, lanes 11, 12, 14, and 15).

To demonstrate the presence of Op*M*NPV GP64 EFP on BVs produced by vAc^{64Z}-infected $Sf9^{OP64\text{-}6}$ cells, BVs were purified from tissue culture supernatants by sucrose gradient centrifugation and examined by Western blot analysis (Fig. 3B, lanes 2, 4, and 6). As a control, BVs were also purified from tissue culture supernatants of Ac*M*NPV-infected Sf9 cells (Fig. 3B, lanes 1, 3, and 5). Replicate blots were probed with either (i) a MAb that reacts only with the Op*M*NPV GP64 EFP (Fig. 3B, lanes 1 and 2) (OpE4A), (ii) a MAb that reacts with GP64 EFPs of both Op*M*NPV and Ac*M*NPV (Fig. 3B, lanes 3 and 4) (AcV5), or (iii) a MAb that reacts with the P39 capsid protein (Fig. 3B, lanes 5 and 6). GP64 EFP was detected in purified BVs of both Ac*M*NPV and vAc^{64Z} by MAb AcV5 (which cross-reacts with GP64 EFPs of both Ac*M*NPV and Op*M*NPV), and capsid protein P39 was also detected in both BV preparations (Fig. 3B, lanes 3 to 6). Using the Op*M*NPV GP64 EFP-specific MAb (OpE4A), we detected the Op*M*NPV GP64 EFP in purified BVs of vAc^{64Z} (Fig. 3B, lane 2) but not in BVs of Ac*M*NPV (Fig. 3B, lane 1). Thus, vAc^{64Z} BVs produced from $Sf9^{OP64\text{-}6}$ cells contained the Op*M*NPV GP64 EFP protein.

To verify that the infection cycle proceeds normally in vAc^{64Z}-infected cells, the kinetics of the infection cycle were examined by pulse-labeling of proteins (Fig. 3C). In vAc^{64Z}-infected Sf9 cells, the overall pattern of protein synthesis was similar to that in Sf9 cells infected with wild-type Ac*M*NPV. At 24 h p.i., a labeled band of approximately 64 kDa was observed in wild-type-Ac*M*NPV-infected cells but not in vAc^{64Z}-infected cells (Fig. 3C, compare lanes 6 and 7). Because 24 h p.i. is the time of maximal GP64 EFP synthesis in Ac*M*NPV-infected Sf9 cells (20), this 64-kDa band is likely GP64 EFP. Comparison of the temporal progression of infection confirms progression into the late phase between 6 and 12 h p.i. and therefore suggests that the viral infection cycle of vAc^{64Z} is not significantly affected by the lack of GP64 EFP expression.

Because sequences flanking the *gp64 efp* genes of Ac*M*NPV

FIG. 4. Role of GP64 EFP in cell-to-cell transmission in cell culture. Sf9 cells were infected at a low MOI (0.1) with either a virus containing an inactivated *gp64 efp* gene (vAc^{64Z}) (A to C) or a control virus expressing β-galactosidase from the *hsp70* promoter (vAc^{hsZ}) (D to F). To identify infected cells, β-galactosidase activity was detected. Cells were fixed with glutaraldehyde and stained with X-Gal at 20 h p.i. (A and D), 48 h p.i. (B and E), or 72 h p.i. (C and F).

and Op*M*NPV are present in the recombinant virus vAc^{64Z} and in the $Sf9^{OP64\text{-}6}$ cell line, respectively, and the two genes are highly similar (3), there exists the formal possibility that recombination between the heterologous genes in the virus and the cell line might result in replacement of the *gp64-lacZ* fusion gene with a functional (Op*M*NPV) *gp64 efp* gene. In addition, selection pressure might force integration of the Op*M*NPV *gp64 efp* gene at random sites within the genome. Such recombination products were not detected in DNA from the vAc^{64Z} viral stocks, using PCR amplification with primers specific for the Op*M*NPV *gp64 efp* gene (data not shown). In control experiments, Op*M*NPV viral DNA was detectable with the Op*M*NPV-specific primers when mixed with Ac*M*NPV DNA at a molar ratio of 1 part Op*M*NPV DNA to 10^4 parts Ac*M*NPV DNA, but it was not detectable at $1{:}10^5$. Our inability to detect Op*M*NPV *gp64 efp* in vAc^{64Z} viral stocks therefore indicates that if any recombinant viruses carrying the Op*M*NPV *gp64 efp* gene were present, they occurred at a frequency of less than 1 in 10^4 particles. Because the most likely recombination events that might restore the *gp64 efp* gene would also remove the *lacZ* gene, expression of the *lacZ* marker gene was used as the indicator of infection in subsequent analyses of vAc^{64Z} infectivity.

Cell-to-cell transmission. To determine if GP64 EFP is required for the production of infectious virions and cell-to-cell transmission of the virus, Sf9 cells were infected at a low MOI (0.1) with vAc^{64Z} or with a *lacZ*-marked control virus (vAc^{hsZ}). At various times p.i., the cells were fixed and stained with X-Gal to detect spread of the *lacZ*-marked viruses from the initially infected cells (Fig. 4). At 20 h p.i., single infected cells were detected in the cultures infected with vAc^{64Z} (Fig. 4A) or with the control virus (Fig. 4D). At 48 h p.i. the control virus had spread from the initially infected cells, resulting in large clusters of infected cells (Fig. 4E), and by 72 h p.i. the control virus had infected most or all cells in the culture (Fig. 4F). In contrast, cultures infected with vAc^{64Z} showed no evidence of cell-to-cell movement, with only single infected cells detected at 48 and 72 h p.i. (Fig. 4B and C, respectively). Thus, these data indicate that GP64 EFP is required for the production of infectious virions and for cell-to-cell movement in cell culture.

To examine the role of GP64 EFP during infection in the animal, vAc^{64Z} occlusion bodies were purified from infected $Sf9^{OP64\text{-}6}$ cells and fed to early-fourth-instar *T. ni* larvae (1.5 to 2 h postmolt). As a control, a second group of larvae was fed occlusion bodies from the *lacZ*-marked control virus (vAc^{hsZ}). At various times postfeeding, animals were dissected and fixed, and infected cells were identified by whole-mount X-Gal staining (Fig. 5). Infected cells in the midgut epithelium were detected at 4 h postfeeding in five of six animals fed vAc^{64Z} occlusion bodies and in five of six animals fed vAc^{hsZ} occlusion bodies (data not shown). By 24 h postfeeding, many midgut cells contained β-galactosidase activity in animals fed either vAc^{64Z} occlusion bodies (Fig. 5A) (three of five animals) or vAc^{hsZ} occlusion bodies (Fig. 5C) (four of five animals), indicating infection. By 4 days postfeeding, all animals fed the control virus vAc^{hsZ} were quiescent and moribund (five of five animals). After X-Gal staining, these animals exhibited extensive β-galactosidase staining in many tissues, indicating systemic infection (Fig. 5D). In parallel experiments, all animals fed vAc^{hsZ} occlusion bodies underwent tissue liquification (typical of late-stage infection by nuclear polyhedrosis viruses) by 5 days postfeeding. In contrast, animals fed vAc^{64Z} occlu-

FIG. 5. Role of GP64 EFP in systemic infection in the insect host. Newly molted fourth-instar *T. ni* larvae were fed a suspension of occlusion bodies (1,000 occlusion bodies per μl) from either the GP64 EFP-null virus (vAc^{64Z}) (A and B) or the control virus (vAc^{hsZ}) (C and D). The larvae were dissected, fixed, and stained with X-Gal to detect β-galactosidase expression in infected cells at either 1 day postfeeding (A and C) or 4 days postfeeding (B and D). Infected midgut epithelial cells were observed as blue cells in the midgut at 1 day postfeeding in larvae fed either the GP64 EFP-null virus (A) or the control virus (C). By 4 days, postfeeding, larvae fed vAc^{64Z} appeared healthy, and only occasional infected cells were detected in the midgut epithelium (B [inset is a higher magnification]). The larvae fed the control virus vAc^{hsZ} (D) exhibited widespread systemic infection of many tissues, and this was consistent with their moribund state.

sion bodies appeared healthy at 5 days postfeeding and continued to develop normally. When examined at 4 days postfeeding by X-Gal staining, these animals did not exhibit infection in any tissues, except for occasional isolated midgut cells containing β-galactosidase activity (Fig. 5B, inset). Thus, occluded virions of vAc^{64Z} were infectious to midgut cells and established a primary infection, but the infection by vAc^{64Z} failed to escape the midgut. Thus, GP64 EFP was not required for infection by ODVs but was essential for the escape of the infection from the midgut into the hemocoel.

To further assess the biological effects of GP64 EFP inactivation, we used a sensitive neonate droplet feeding assay to determine the lethality of vAc^{64Z} to neonate larvae (Table 1). *T. ni* neonates were allowed to feed on a suspension of occlusion bodies of either vAc^{64Z} or wild-type Ac*M*NPV. Because each larva typically consumes a volume of 8 to 13 nl (17, 18), occlusion bodies were diluted to a concentration of 1, 5, or 10 occlusion bodies per 10 nl, and neonate larvae were allowed to feed for estimated doses of 1, 5, or 10 occlusion bodies per larva. By 4 days p.i., neonates fed 5 or 10 occlusion bodies of wild-type Ac*M*NPV exhibited 80 and 93% mortality, respectively, while larvae fed an average of 1 occlusion body of wild-type Ac*M*NPV exhibited 30% mortality (Table 1, experiment I). These observations are consistent with previously published data for wild-type Ac*M*NPV in the droplet feeding assay (13). In contrast, larvae fed vAc^{64Z} occlusion bodies at doses of one or five occlusion bodies per 10 nl exhibited no virus-induced mortality. In the group of larvae fed 10 vAc^{64Z} occlusion bodies, one animal died, but upon microscopic examination, no evidence of polyhedrosis was found. In a second experiment, doses of 10 occlusion bodies of wild-type Ac*M*NPV per 10 nl resulted in 65% mortality (Table 1, experiment II). However, doses of vAc^{64Z} of as many as 1,000 occlusion bodies per 10 nl (100 times the measured 65% lethal dose of wild-type Ac*M*NPV in this experiment) resulted in no virus-induced mortality by 4 days p.i. Thus, the vAc^{64Z} virus was not lethal to *T. ni* neonate larvae at any dose tested.

TABLE 1. Comparative mortalities of neonates fed vAc^{64Z} and Ac*M*NPV in droplet feeding assays

Expt	Virus	Dose (OBs[a]/10 nl)	*n*	% Mortality
I	Ac*M*NPV	1	30	30.0
		5	30	80.0
		10	30	93.3
	vAc^{64Z}	1	30	0
		5	30	0
		10	30	(3.3)[b]
II	Control	0	57	0
	Ac*M*NPV	0.1	57	1.8
		1	58	20.7
		10	57	65.0
	vAc^{64Z}	10	53	0
		100	55	0
		1,000	52	0

[a] OB, occlusion body.
[b] One animal died, but not because of polyhedrosis.

DISCUSSION

Generation of a virus lacking GP64 EFP. To study the role of the baculovirus GP64 EFP protein in the context of a viral infection, we generated a recombinant baculovirus that contains an insertionally inactivated *gp64 efp* gene and examined the effects of that mutation on viral infectivity and on propagation of the virus in cell culture and in animals. Previous studies of the GP64 EFP protein demonstrated that some anti-GP64 antibodies are capable of neutralizing the infectivity of the virus (15, 25, 28, 38). Because of the likelihood that

inactivation of the *gp64 efp* gene would be difficult, we chose to supply the GP64 EFP protein in *trans*, from a stably transfected cell line, and to then use homologous recombination for generating an inactivated *gp64 efp* gene in the context of an otherwise wild-type Ac*M*NPV baculovirus.

One disadvantage of this approach is that if the *gp64 efp* gene is essential, a very strong selection pressure for regenerating a GP64 EFP$^+$ virus may result in recombination between the virus and the *gp64 efp* gene within the cell line. To reduce this possibility and ensure that we examined only virus containing the inactivated *gp64 efp* gene, we used the following strategies: (i) for generating the stably transfected cell line, we selected a heterologous *gp64 efp* gene (derived from a different baculovirus, Op*M*NPV); (ii) recombinant vAc^{64Z} virus stocks were screened by restriction analysis, Western blots, and PCR for significant levels of any revertant virus; and (iii) a *lacZ* marker gene was fused in frame with the wild-type Ac*M*NPV *gp64 efp* gene, and analyses of the loss-of-function phenotype of the recombinant virus relied on detection of the β-galactosidase marker. Thus, the analysis of only cells expressing the *lacZ* marker gene ensured that we exclusively analyzed viruses carrying the inactivated *gp64 efp* gene.

Constitutive expression of GP64 EFP on Sf9^{OP64-6} cells. The first step in the above-described strategy involved the production of cell lines that constitutively expressed the GP64 EFP protein from Op*M*NPV. In addition to facilitating the construction of the recombinant virus, the use of a heterologous *gp64 efp* gene also allowed us to determine whether the highly conserved (but not identical) Op*M*NPV GP64 EFP could functionally replace the Ac*M*NPV GP64 EFP protein. After constructing the Op*M*NPV GP64 EFP-expressing cell lines, we performed several quantitative studies to compare GP64 EFP expression from Ac*M*NPV-infected cells, stably transfected cells, and transiently transfected cells. For one aspect of these studies, we measured the quantities of GP64 EFP expressed on a per-cell basis. At 24 h p.i., Ac*M*NPV-infected Sf9 cells contained on average approximately 3.9×10^6 molecules of GP64 EFP per cell (equivalent to 1.3×10^6 trimers per cell). Stably transfected Sf9^{OP64-6} cells contained only approximately 7.6×10^5 molecules (equivalent to 2.5×10^5 trimers) of GP64 EFP per cell. While the total quantity of GP64 EFP per infected cell was approximately five times higher than the quantity detected per Sf9^{OP64-6} cell, a further (CELISA) analysis of the average levels of GP64 EFP at the surface of these cells indicated that the level of GP64 EFP at the surface of the Sf9^{OP64-6} cells was similar to that at the surface of infected cells. Flow cytometry analysis of surface GP64 EFP levels on individual cells in each population indicated that there was less cell-to-cell variability among Ac*M*NPV-infected cells than among Sf9^{OP64-6} cells. Greater variability of GP64 EFP surface density appeared to be a general feature of transfected cells, since both the Sf9^{OP64-2} cell line and transiently transfected cells also exhibited wider variations in GP64 EFP surface levels. The narrower range of GP64 EFP surface levels in infected Sf9 cells is likely due to the synchronization of GP64 EFP expression during infection, since at 24 h p.i., GP64 EFP expression is primarily from the late promoter. In contrast, GP64 EFP in transfected cells results from constitutive expression by the early promoter and accumulation of the protein in a population of asynchronously dividing cells. In transient transfections, variable levels of GP64 EFP expression may also arise from cell-to-cell variations in DNA uptake during transfection.

Because cell surface levels of GP64 EFP from infected and Sf9^{OP64-6} cells were similar, and yet an approximately fivefold difference in the total quantity of GP64 EFP was detected, these data suggest that no more than 20% of the total GP64 EFP protein detected in Ac*M*NPV-infected Sf9 cells (at 24 h p.i.) is found at the cell surface. Using this estimate of surface localization (20%) in combination with quantitative ECL data derived from whole-cell measurements of GP64 EFP, we estimate that Ac*M*NPV-infected Sf9 cells (MOI of 10, 24 h p.i.) contain an average surface density of 2.6×10^5 trimers of GP64 EFP per cell, at most. These preliminary studies suggested that the Sf9^{OP64-6} cell line produces sufficient quantities of surface localized GP64 EFP to yield reasonable titers of BVs when infected by a virus lacking a *gp64 efp* gene. Production of infectious vAc^{64Z} BV from Sf9^{OP64-6} cells was on the order of 2×10^7 to 3×10^7 infectious units per ml (determined from the 50% tissue culture infective dose [$TCID_{50}$] on Sf9^{OP64-6} cells). The presence of GP64 EFP on the surface of the Sf9^{OP64-6} cells apparently did not interfere with infection, since the $TCID_{50}$ titer of the wild-type Ac*M*NPV stock determined on the Sf9^{OP64-6} cells was approximately 1.3-fold higher than the titer determined on Sf9 cells. In addition to being useful for production of recombinant baculoviruses containing deletions or mutations in GP64 EFP, these stably transfected cell lines constitutively expressing GP64 EFP will also be useful for studies of GP64 EFP-mediated membrane fusion.

***gp64 efp* is an essential baculovirus gene.** The production of infectious BVs by vAc^{64Z}-infected Sf9^{OP64-6} cells demonstrates that the Op*M*NPV GP64 EFP can functionally substitute for the Ac*M*NPV GP64 EFP in the production of BVs. In addition, vAc^{64Z} virions (produced in Sf9^{OP64-6} cells) were infectious to Sf9 cells, indicating that this aspect of host range was apparently unaffected. Thus, the GP64 EFP proteins from these two related baculoviruses appear to be interchangeable. Of particular importance, we demonstrated that vAc^{64Z} BVs produced in Sf9^{OP64-6} cells are able to enter and infect Sf9 cells, but in the absence of the *gp64 efp* gene, the vAc^{64Z} virus is unable to transmit the infection to uninfected neighboring cells. Thus, *gp64 efp* is an essential baculovirus gene, and the GP64 EFP protein is required for the cell-to-cell transmission of the infection. Studies to identify the cause of the defect in viral transmission are now in progress. Preliminary studies suggest that virion budding is defective in the absence of GP64 EFP.

GP64 EFP is not essential for infectivity of occluded virions. In previous studies, the transmission of virus from the midgut to the hemocoel has been studied by using marker genes to follow the progression of tissues infected (9, 10). Virions budding from the basal side of the midgut epithelial cells have been observed (12), and virion budding is believed to serve as the primary mode of viral movement from the midgut epithelium to the hemocoel. Hemocytes (22), cells of the tracheal system (9), and basal lamina-associated muscle and tracheal cells (10) have been proposed as the primary cells infected after the first round of replication in midgut epithelial cells. It has also recently been suggested that the tracheal system may serve as a conduit for BV transmission across the basal lamina of the midgut epithelium to other tissues within the hemocoel (9).

In the current study, we examined the role of GP64 EFP during infection in the animal by feeding occlusion bodies prepared from vAc^{64Z}-infected cells to either neonate or early-fourth-instar *T. ni* larvae. Using whole-mount histological staining of fourth-instar *T. ni* larvae to detect infection, we found that the vAc^{64Z} ODVs were capable of infecting cells of the midgut epithelium, but infection by vAc^{64Z} did not move beyond the midgut. The ability of vAc^{64Z} to produce infectious occluded virions in the absence of GP64 EFP expression is consistent with previous studies that found no detectable GP64 EFP protein associated with the occluded virus (3, 6, 15), and

it clearly demonstrates the virion phenotype specificity of the GP64 EFP protein.

As perhaps the most sensitive indicator of systemic propagation of viral infection, we examined mortality in neonate larvae fed occlusion bodies of vAc^{64Z}. At doses of up to 100 times the 65% lethal dose of Ac*M*NPV, the vAc^{64Z} virus was nonlethal to *T. ni* neonates. The lack of vAc^{64Z}-induced mortality in *T. ni* neonate larvae thus confirms the observations in tissues of whole fourth-instar larvae and demonstrates that the inability of the vAc^{64Z} virus to escape from the midgut epithelium results in a nonlethal infection in the animal. These results therefore demonstrate an absolute requirement for GP64 EFP in the progression of the infection from the midgut epithelium to the systemic form of the disease in tissues of the hemocoel.

ACKNOWLEDGMENTS

We thank P. R. Roelvink for providing the control virus vAc^{hsZ}, R. R. Granados and K. McKenna for providing larvae and for assistance with the neonate assays, D. Theilman for providing the *lacZ* cassette, and J. R. Manning for kindly providing anti-P39 MAb 39.

This research was supported by NIH grants AI 33657 and AI 31130 and by Boyce Thompson Institute projects 1250-01 and 1255-17.

REFERENCES

1. **Ayres, M. D., S. C. Howard, J. Kuzio, M. Lopez-Ferber, and R. D. Possee.** 1994. The complete DNA sequence of *Autographa californica* nuclear polyhedrosis virus. Virology **202:**586–605.
2. **Blissard, G. W., P. H. Kogan, R. Wei, and G. F. Rohrmann.** 1992. A synthetic early promoter from a baculovirus: roles of the TATA box and conserved start site CAGT sequence in basal levels of transcription. Virology **190:**783–793.
3. **Blissard, G. W., and G. F. Rohrmann.** 1989. Location, sequence, transcriptional mapping, and temporal expression of the *gp64* envelope glycoprotein gene of the *Orgyia pseudotsugata* multicapsid nuclear polyhedrosis virus. Virology **170:**537–555.
4. **Blissard, G. W., and G. F. Rohrmann.** 1991. Baculovirus *gp64* gene expression: analysis of sequences modulating early transcription and transactivation by IE1. J. Virol. **65:**5820–5827.
5. **Blissard, G. W., and J. R. Wenz.** 1992. Baculovirus GP64 envelope glycoprotein is sufficient to mediate pH-dependent membrane fusion. J. Virol. **66:**6829–6835.
6. **Braunagel, S. C., and M. D. Summers.** 1994. Autographa californica nuclear polyhedrosis virus, PDV, and ECV viral envelopes and nucleocapsids: structural proteins, antigens, lipid and fatty acid profiles. Virology **202:**315–328.
7. **Casadaban, M. J. J., A. Martinez-Arias, S. K. Shapira, and J. Chou.** 1981. Beta-galactosidase gene fusions for analyzing gene expression in Escherichia coli and yeast. Methods Enzymol. **100:**293–308.
8. **Chernomordik, L., E. Leikina, M. Cho, and J. Zimmerberg.** 1995. Control of baculovirus gp64-induced syncytium formation by membrane lipid composition. J. Virol. **69:**3049–3058.
9. **Engelhard, E. K., L. N. W. Kam-Morgan, J. O. Washburn, and L. E. Volkman.** 1994. The insect tracheal system: a conduit for the systemic spread of *Autographa californica* M nuclear polyhedrosis virus. Proc. Natl. Acad. Sci. USA **91:**3224–3227.
10. **Flipsen, J. T. M., J. W. M. Martens, M. M. Van-Oers, J. M. Vlak, and J. W. M. Van-Lent.** 1995. Passage of *Autographa californica* nuclear polyhedrosis virus through the midgut epithelium of *Spodoptera exigua* larvae. Virology **208:**328–335.
11. **Gill, S. C., and P. H. von Hippel.** 1989. Calculation of protein extinction coefficients from amino acid data. Anal. Biochem. **182:**319–326.
12. **Granados, R. R., and K. A. Lawler.** 1981. In vivo pathway of *Autographa californica* baculovirus invasion and infection. Virology **108:**297–308.
13. **Greenspan, G. L., B. G. Corsaro, P. R. Hughes, and R. R. Granados.** 1991. In-vivo enhancement of baculovirus infection by the viral enhancing factor of a granulosis virus of the cabbage looper trichoplusiani-lepidoptera noctuidae. J. Invert. Pathol. **58:**203–210.
14. **Hink, W. F.** 1970. Established insect cell line from the cabbage looper, *Trichoplusia ni*. Nature (London) **226:**466–467.
15. **Hohmann, A. W., and P. Faulkner.** 1983. Monoclonal antibodies to baculovirus structural proteins: determination of specificities by Western blot analysis. Virology **125:**432–444.
16. **Horton, H. M., and J. P. Burand.** 1993. Saturable attachment sites for polyhedron-derived baculovirus on insect cells and evidence for entry via direct membrane fusion. J. Virol. **67:**1860–1868.
17. **Hughes, P. R., N. A. M. van Beek, and H. A. Wood.** 1986. A modified droplet feeding method for rapid assay of Bacillus thuringiensis and baculoviruses in Noctuid larvae. J. Invert. Pathol. **48:**187–192.
18. **Hughes, P. R., and H. A. Wood.** 1981. A synchronous peroral technique for the bioassay of insect viruses. J. Invert. Pathol. **37:**154–159.
19. **Jarvis, D. L., J. A. G. W. Fleming, G. R. Kovacs, M. D. Summers, and L. A. Guarino.** 1990. Use of early baculovirus promoters for continuous expression and efficient processing of foreign gene products in stably transformed lepidopteran cells. Bio/Technology **8:**950–955.
20. **Jarvis, D. L., and A. Garcia.** 1994. Biosynthesis and processing of the *Autographa californica* nuclear polyhedrosis virus gp64 protein. Virology **205:**300–313.
21. **Jarvis, D. L., and L. A. Guarino.** 1995. Continuous foreign gene expression in transformed Lepidopteran insect cells, p. 187–202. *In* C. Richardson (ed.), Methods in molecular biology, vol. 39. Baculovirus expression protocols. Humana Press Inc., Totowa, N.J.
22. **Keddie, B. A., G. W. Aponte, and L. E. Volkman.** 1989. The pathway of infection of *Autographa californica* nuclear polyhedrosis virus in an insect host. Science **243:**1728–1730.
23. **Kogan, P. H., and G. W. Blissard.** 1994. A baculovirus *gp64* early promoter is activated by host transcription factor binding to CACGTG and GATA elements. J. Virol. **68:**813–822.
24. **Kogan, P. H., X. Chen, and G. W. Blissard.** 1995. Overlapping TATA-dependent and TATA-independent early promoter activities in the baculovirus *gp64 envelope fusion protein* gene. J. Virol. **69:**1452–1461.

24a. **Kuzio, J.** Personal communication.

25. **Monsma, S. A., and G. W. Blissard.** 1995. Identification of a membrane fusion domain and an oligomerization domain in the baculovirus GP64 envelope fusion protein. J. Virol. **69:**2583–2595.
26. **Oomens, A. G. P., S. A. Monsma, and G. W. Blissard.** 1995. The baculovirus GP64 envelope fusion protein: synthesis, oligomerization, and processing. Virology **209:**592–603.
27. **O'Reilly, D. R., L. K. Miller, and V. A. Luckow.** 1992. Baculovirus expression vectors, a laboratory manual. W. H. Freeman & Co., New York.
28. **Roberts, S. R., and J. S. Manning.** 1993. The major envelope glycoprotein of the extracellular virion of *Autographa californica* nuclear polyhedrosis virus possesses at least three distinct neutralizing epitopes. Virus Res. **28:**285–297.
29. **Roberts, T. E., and P. Faulkner.** 1989. Fatty acid acylation of the 67K envelope glycoprotein of a baculovirus *Autographa californica* nuclear polyhedrosis virus. Virology **172:**377–381.
30. **Smith, G. E., and M. D. Summers.** 1978. Analysis of baculovirus genomes with restriction endonucleases. Virology **89:**517–527.
31. **Southern, P. J., and P. Berg.** 1982. Transformation of mammalian cells to antibiotic resistance with a bacterial gene under control of the SV40 early region promoter. J. Mol. Appl. Genet. **1:**327–341.
32. **Summers, M. D., and G. E. Smith.** 1987. A manual of methods for baculovirus vectors and insect cell culture procedures. Texas Agricultural Experiment Station bulletin no. 1555. Texas Agricultural Experiment Station, College Station.
33. **Sussman, D. J.** 1995. 24-hour assay for estimating the titer of beta-galactosidase expressing baculovirus. BioTechniques **18:**50–51.
34. **Vlak, J. M., A. Schouten, M. Usmany, G. J. Belsham, E. C. Klinge Roode, A. J. Maule, J. W. M. Van Lent, and D. Zuidema.** 1990. Expression of cauliflower mosaic virus gene I using a baculovirus vector based upon the P10 gene and a novel selection method. Virology **179:**312–320.
35. **Volkman, L. E., and P. A. Goldsmith.** 1984. Budded *Autographa californica* NPV 64K protein: further biochemical analysis and effects of postimmunoprecipitation sample preparation conditions. Virology **139:**295–302.
36. **Volkman, L. E., and P. A. Goldsmith.** 1985. Mechanism of neutralization of budded *Autographa californica* nuclear polyhedrosis virus by a monoclonal antibody: inhibition of entry by adsorptive endocytosis. Virology **143:**185–195.
37. **Volkman, L. E., and P. A. Goldsmith.** 1988. Resistance of the 64K protein of budded Autographa californica nuclear polyhedrosis virus to functional inactivation by proteolysis. Virology **166:**285–289.
38. **Volkman, L. E., P. A. Goldsmith, R. T. Hess, and P. Faulkner.** 1984. Neutralization of budded *Autographa californica* NPV by a monoclonal antibody: identification of the target antigen. Virology **133:**354–362.
39. **Volkman, L. E., and M. D. Summers.** 1977. *Autographa californica* nuclear polyhedrosis virus: comparative infectivity of the occluded, alkali-liberated, and nonoccluded forms. J. Invert. Pathol. **30:**102–103.
40. **Volkman, L. E., M. D. Summers, and C. H. Hsieh.** 1976. Occluded and nonoccluded nuclear polyhedrosis virus grown in *Trichoplusia ni*: comparative neutralization, comparative infectivity, and in vitro growth studies. J. Virol. **19:**820–832.
41. **Whitford, M., S. Stewart, J. Kuzio, and P. Faulkner.** 1989. Identification and sequence analysis of a gene encoding gp67, an abundant envelope glycoprotein of the baculovirus *Autographa californica* nuclear polyhedrosis virus. J. Virol. **63:**1393–1399.
42. **Whitt, M. A., and J. S. Manning.** 1988. A phosphorylated 34-kDa protein and a subpopulation of polyhedrin are thiol linked to the carbohydrate layer surrounding a baculovirus occlusion body. Virology **163:**33–42.

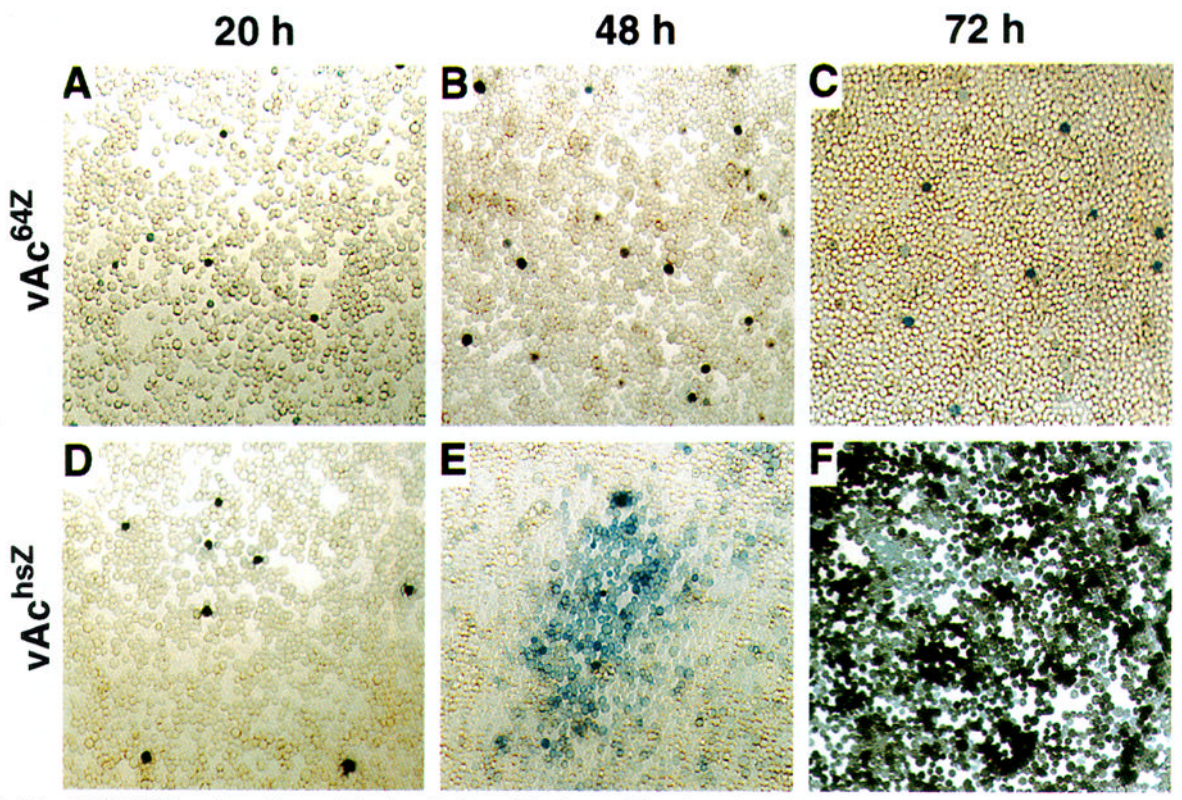
20 h
48 h
72 h
A
B
C
D
E
F
vAc64Z
vAchsZ

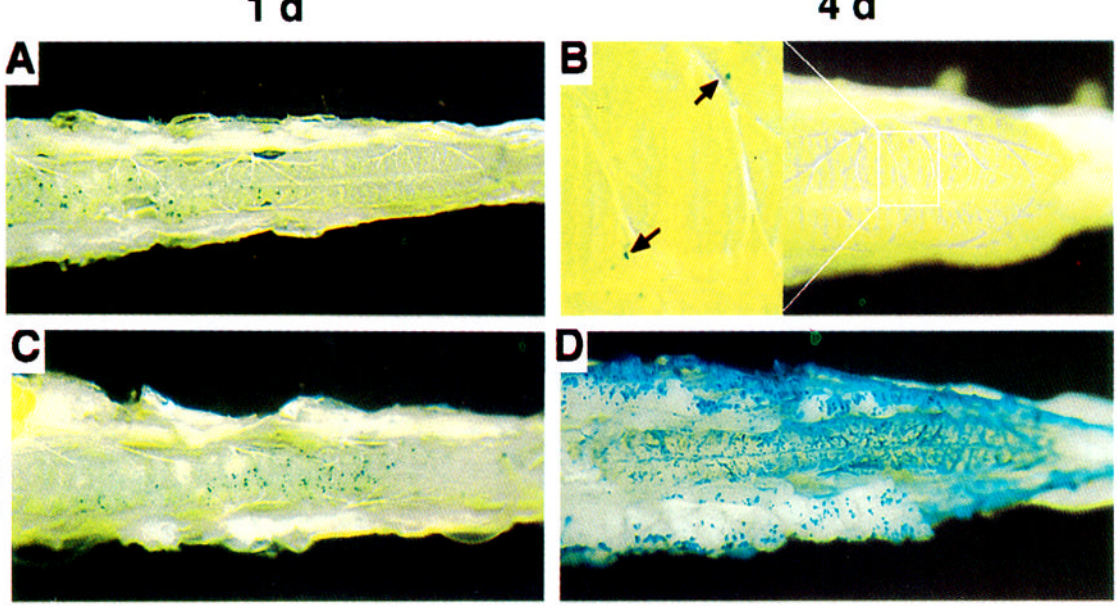
1 d
4 d
A
B
C
D
vAc64Z
vAchsZ